ORIGINAL RESEARCH

Non-invasive continuous respiratory monitoring using temperature-based sensors

Daniel E. Hurtado[1] · Angel Abusleme[2] · Javier A. P. Chávez[3]

Abstract

Respiratory rate (RR) is a key vital sign that has been traditionally employed in the clinical assessment of patients and in the prevention of respiratory compromise. Despite its relevance, current practice for monitoring RR in non-intubated patients strongly relies on visual counting, which delivers an intermittent and error-prone assessment of the respiratory status. Here, we present a novel non-invasive respiratory monitor that continuously measures the RR in human subjects. The respiratory activity of the user is inferred by sensing the thermal transfer between the breathing airflow and a temperature sensor placed between the nose and the mouth. The performance of the respiratory monitor is assessed through respiratory experiments performed on healthy subjects. Under spontaneous breathing, the mean RR difference between our respiratory monitor and visual counting was 0.4 breaths per minute (BPM), with a 95% confidence interval equal to [− 0.5, 1.3] BPM. The robustness of the respiratory sensor to the position is assessed by studying the signal-to-noise ratio in different locations on the upper lip, displaying a markedly better performance than traditional thermal sensors used for respiratory airflow measurements.

Keywords Monitoring · Respiration · Thermal sensors

1 Introduction

Continuous non-invasive respiratory monitoring has gained renewed interest in hospital settings such as the post-anesthesia care unit (PACU), the intensive care unit, and the general floor, as it can provide early warnings and alerts of respiratory compromise in non-intubated patients [4, 21]. Respiratory rate (RR) is a key vital sign that has long been used as a primary parameter in the evaluation of the health condition of a patient [11]. In particular, RR plays a key role in the prevention and management of postoperative opioid-induced respiratory depression, a life-threatening condition that can occur in patients undergoing pain-management treatments based on opioids who present low RR [5, 12]. The prevention of respiratory compromise has been recognized as a priority by the Joint Commission, highlighting the relevance of developing reliable and cost-effective respiratory monitoring systems for RR [15].

Despite the importance of continuously monitoring RR in hospital patients, the current standard of care for assessing the respiratory condition largely relies on visual counting, which leads to an intermittent and inaccurate measurement of RR [10]. Pulse oximeters have been traditionally used to assess the respiratory condition of patients, and have gained their popularity based on their non-invasiveness, cost-effectiveness and worldwide availability [6]. However, pulse oximeters can be late in the detection of respiratory depression, as in such condition they measure the decrease of peripheral bloodstream oxygenation, which is known to be a late symptom of respiratory compromise [21]. Advanced signal processing from photopletismography has been recently develop to deliver a continuous estimate of RR [2]. A more accurate non-invasive approach to respiratory monitoring are systems based on measuring changes of thoracic electrical impedance. Some impedance-based systems have the advantage of delivering not only RR but also other important ventilatory

✉ Daniel E. Hurtado
  dhurtado@ing.puc.cl

1   Department of Structural and Geotechnical Engineering, School of Engineering, and Institute for Biological and Medical Engineering, Schools of Engineering, Medicine and Biological Sciences, Pontificia Universidad Católica de Chile, Vicuña Mackenna 4860, Santiago, Chile

2   Department of Electrical Engineering, School of Engineering, Pontificia Universidad Católica de Chile, Vicuña Mackenna, 4860 Santiago, Chile

3   DICTUC S.A., Vicuña Mackenna, 4860 Santiago, Chile

parameters such as minute ventilation [3, 19]. Impedance-based respiratory monitors, however, have the disadvantage of being inaccurate in detecting RR in the low-frequency range, as well as being subject to motion artifacts [6]. RR continuous estimates based on the motion of the chest and abdomen have also been estimated using piezoelectric sensing devices [13].

An alternative method to monitor respiratory activity is the use acoustic transducers attached to the throat of patients. Acoustic signals acquired are then filtered, from which RR can be determined with high accuracy [8, 17]. However, noise coming from the environment or from the patient when he or she coughs, sneezes, snores or cries can decrease the performance of respiratory monitors based on acoustic sensors [7]. More recently, optical cameras and radars have been used to contactless monitor the respiratory activity. Using a camera and image processing, RR has been inferred by determining the changes in color of the skin of patients [18], which has also been studied by analyzing temperature changes in thermal images from infrared thermal cameras [9]. RR can also be determined from chest motion by tracking pixels trajectories from camera images [14] as well as using radar technology [20]. While these methods provide a novel contactless alternative to standard monitoring systems, they can be sensitive to involuntary body motions, and their estimates can be hindered in the hospital setting when people or objects block the space between the device and the chest of the patient.

In this paper, we present a novel continuous and non-invasive temperature respiratory monitoring system (TRMS) for RR. Nasal and oral respiratory flow is derived from analyzing temperature changes occurring at the respiratory sensor, and then used to estimate the RR. We test the accuracy and robustness of the system in the estimation of RR under different guided and spontaneous respiratory settings in normal volunteers.

2 Materials and methods

2.1 Description of the monitoring system

The temperature-based respiratory monitoring system consists of a respiratory sensor, and an external monitor, where respiratory signal, respiratory frequency and other flow parameters are displayed. The respiratory sensor is a wearable, lightweight, non-invasive device that adheres to the skin below the nose and above the upper lip of the subject. It measures the thermal component of the user's respiration gas flow and transforms temperature into an electrical signal, which is processed and sent to the external monitor. An isometric view of the sensor is included in Fig. 1. The sensor includes one housing made of plastic
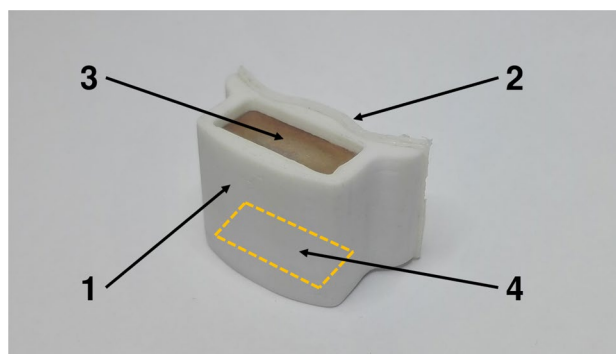

Fig. 1 Isometric view of the respiratory sensor: (1) Case, (2) Flexible support, (3) Nasal heat concentrator, (4) Oral heat concentrator

material with low thermal conductivity. The fixation of the sensor to the user skin is materialized either through an medical-grade adhesive sticker placed in the surface that is in contact with the skin. The dimensions of the sensor (length × width × height) are 30 mm × 16 mm × 20 mm and the weight is 8 g.

Nasal and oral thermal collectors made of copper are installed in the housing surface facing nasal and oral flow. Thermal collectors transfer the heat coming from the respiration gas flow to temperature sensors, placed inside the housing and in contact with the collectors. Temperature changes of the respiratory flowing gas will result in proportional changes in the thermal sensor resistance, which are transformed into continuous electrical signals that are transferred to the external monitor for further processing. An analog-to-digital converter (ADC) integrated in a microcontroller within the external monitor converts the analog voltage signal into digital data (10-bit resolution and 100-S/s sampling rate), which is then processed to obtain the relevant respiratory flow parameters.

To estimate the RR the nasal and oral signals are added, and a mean-crossing algorithm is employed. Mean-crossing algorithms generally results in accurate estimates both for low and high frequencies [16]. Figure 2 shows how RR is computed using a representative graphical example. We use a time window of 30 s to compute the mean respiratory cycles periods, in order to estimate the mean respiratory rate. After signal processing, the respiratory signal is graphically displayed in the screen of the external monitor, along with the RR.

2.2 Position sensitivity and human breathing tests

Twenty healthy subjects, ten females and ten males, were recruited for this study and underwent a protocol approved by the institutional ethics committee of the Pontificia Universidad Católica de Chile. Inclusion criteria were: volunteers with age between 18 and 65 y old, non-smokers, no
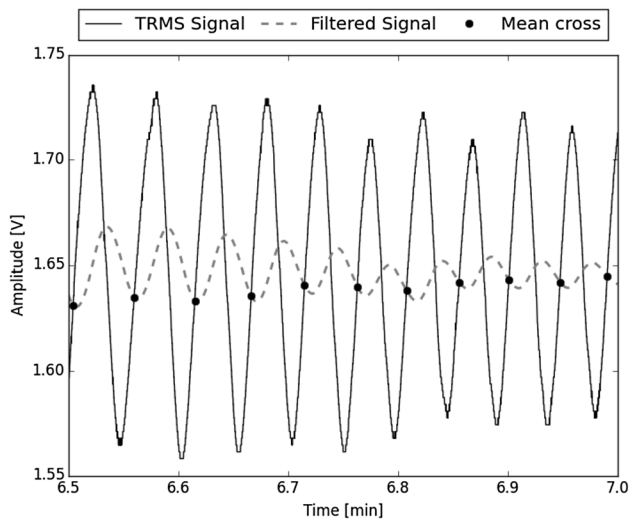
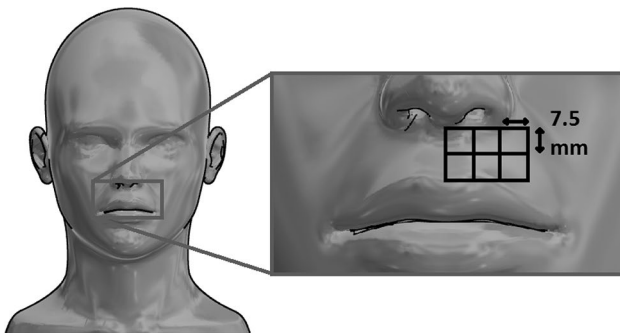**Fig. 2** RR estimation using a mean-crossing algorithm

Fig. 3 Grid and position markers for the sensitivity test

record of chronic pulmonary disease, and no allergies to copper. The breathing sensor was installed in all subjects, and the respiratory signal was continuously measured during the whole duration of the study. Additionally, a pulse oximeter (Particle sensor, MAX30105, Sparkfun, Niwot, Colorado, USA) was installed on all the subjects to continuously record the peripheral oxygen saturation (SpO2). During the experiment, visual counting of respiratory cycles was electronically recorded by means of a push-button counter controlled by an expert, which was considered the gold standard for the purpose of method comparison and error analysis. All subjects were requested to lay down on a stretcher in supine position.

To test the sensitivity of the sensor to the position, we acquired respiratory signals at several positions in a grid marked on the face of one volunteer, as shown in Fig. 3. The grid spacing was 7.5 mm both in the horizontal and vertical directions. The subject breathing was guided by a metronome set at 6 and 15 BPM for a period of 1 min. Respiratory flow signals acquired by the sensor were then processed to

compute the RR in a continuous way, and signal-to-noise ratio (SNR). The protocol was repeated on the same subject using a thermistor instead of the TRMS (NTC 10k thermistor, Vishay Components, Malvern, Pennsylvania, USA), for which the same outputs were recorded, in order to compare both performances.

Several human breathing tests were performed on all volunteers as part of the experimental protocol. First, subjects were asked to breath through their nose for one minute following a metronome at rates 6, 8 and 10 BPM. This experiment was then repeated for oral breathing, with nasal flow blocked by using nose pins. Second, subjects were asked to rest and breath spontaneously during 10 min. Third, after a period of 1 min of spontaneous breathing, subjects were asked to hold their breath as long as it was comfortable for them. Finally, after a second period of one min of normal breathing, subjects were asked to breath against a closed glottis for as long a they could, to simulate obstructed breathing situations.

2.3 Statistical analysis

The RR signal delivered by the monitoring system was compared to the gold standard. The relative error for the moving time window i was calculated as

$$Error_i\,[\%] = \frac{RR_{i,TRMS} - RR_{i,ref}}{\frac{1}{2}(RR_{i,TRMS} + RR_{i,ref})} \tag{1}$$

where $RR_{i,ref}$ is the reference value of RR obtained from visual counting, and $RR_{i,TRMS}$ is the RR obtained from the TRMS. The bias is defined as the average of the set of relative errors ($i = 1, ..., N_{windows}$), the precision is the standard deviation of the set of relative errors, and the accuracy is defined as the root-mean-square value of the relative error set.

3 Results

The SNR was computed for all locations in the grid considered in the position sensitivity study. Continuous maps were generated, by means of interpolation, for the cases of guided RR = 6 BPM (Fig. 4a) and guided RR = 15 BPM (Fig. 4b), both for the thermistor and the TRMS. A solid line is plotted in all figures for the level set where SNR = 0, indicating regions where the signal and the noise have the same amplitude. In both cases, the SNR distribution in the case of the TRMS was positive for practically the entire spatial domain considered in the study. In contrast, the thermistor had positive SNR values close to the nostrils, and quickly decayed as it was located farther away.
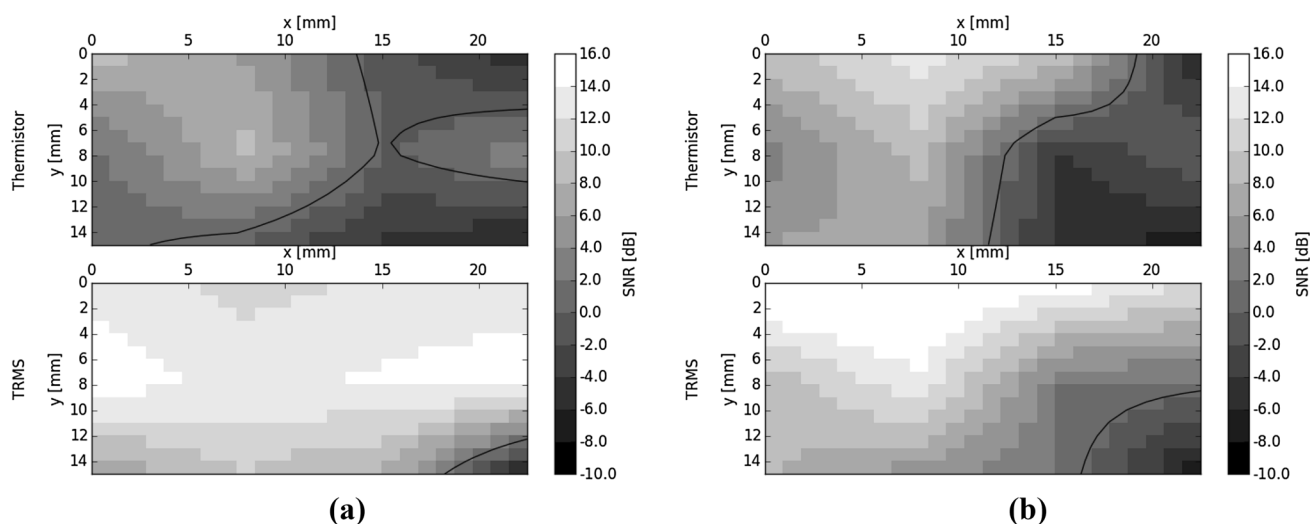
Fig. 4 Signal-to-noise ratio map during sensitivity test. **a** Guided breathing at 6 BPM. **b** Guided breathing at 15 BPM. Solid black line shows the level set that corresponds to SNR = 0 dB

Accuracy of the RR estimated by the TRMS and by a thermistor was computed for all locations in the grid considered in the position sensitivity study. Continuous maps were generated by means of interpolation for the cases of guided RR = 6 BPM (Fig. 5a) and guided RR = 15 BPM (Fig. 5b), both for the thermistor and the TRMS. In the case of the TRMS, the accuracy was less than 5% for most of the area under study, with the exception of a very small region in the bottom right corner. In contrast, the thermistor only achieves accuracy values less than 5% in a reduced region directly under the nostril, out of which accuracy rapidly increases up to values of 40%.

The respiratory signals for one subject under guided and spontaneous breathing are reported in Fig. 6. Bias, precision and accuracy values for the sample group under guided breathing at 6, 8 and 10 BPM are reported in Table 1 for nasal breathing and oral breathing. The mean error for nasal breathing and oral breathing was 0.1 and − 1.6 BPM respectively (Fig. 7). In these controlled experiments, the absolute bias (average error) was less than 0.2 BPM and 2.0 BPM for nasal and oral breathing, respectively. In general, error measures for the case of oral breathing are larger than in the case of nasal breathing.

The time evolution of the RR for a representative subject (subject 10) under spontaneous breathing, measured both
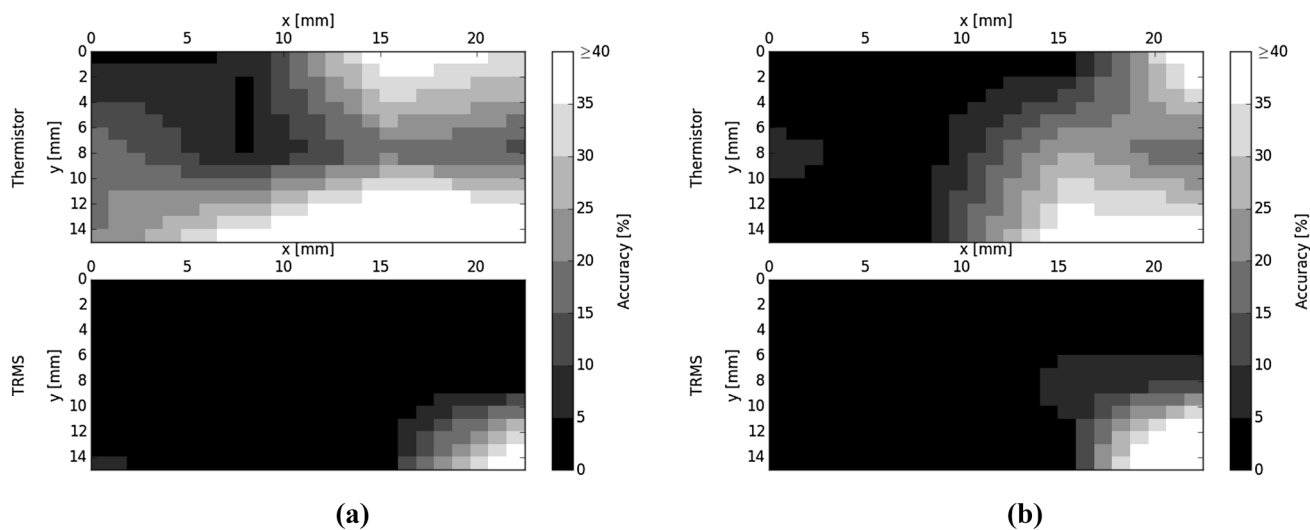

Fig. 5 Accuracy map during sensitivity test. **a** Guided breathing at 6 BPM. **b** Guided breathing at 15 BPM
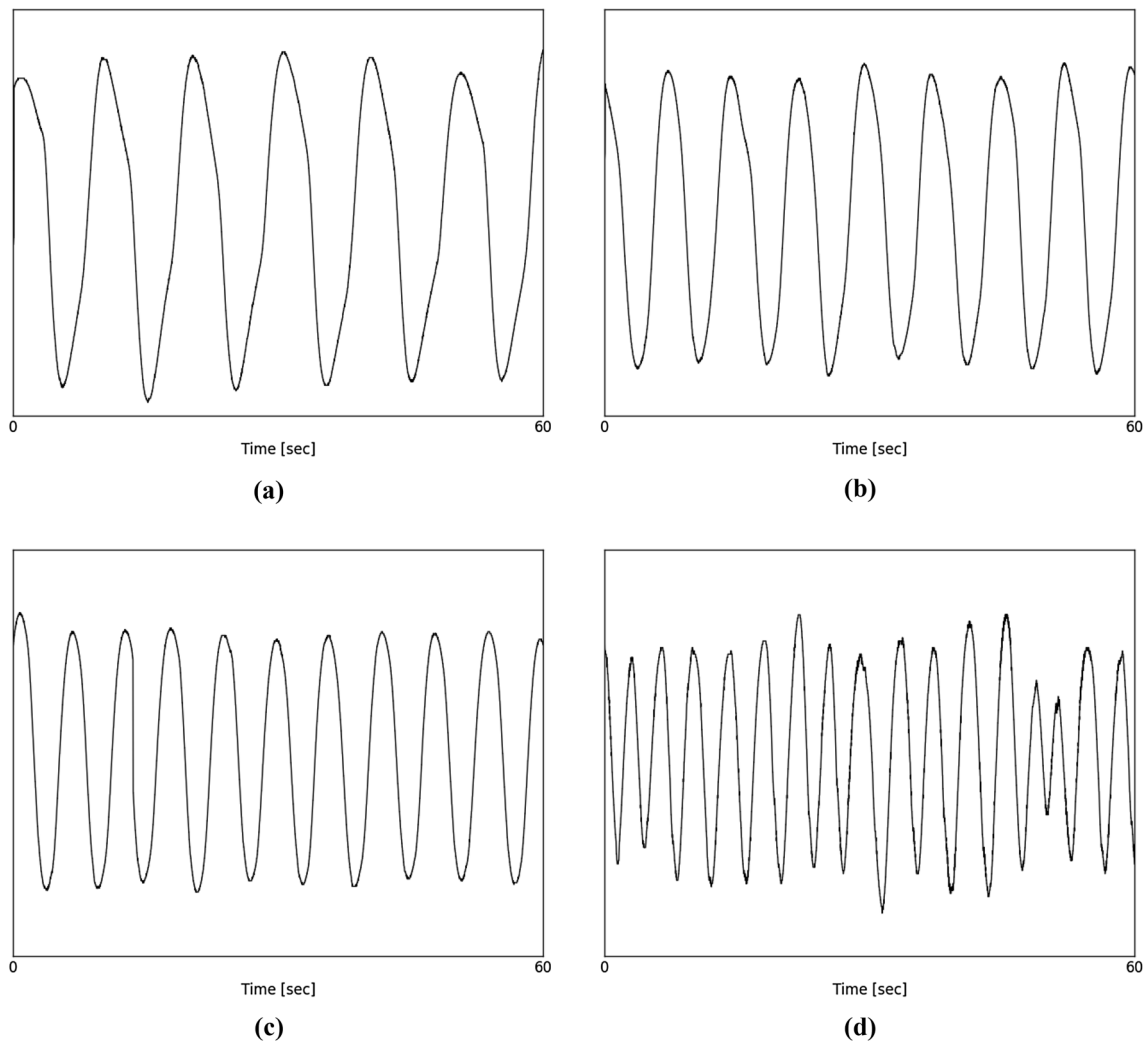
Fig. 6 Respiratory patterns of a volunteer. **a** Guided breathing at 6 BPM. **b** Guided breathing at 8 BPM. **c** Guided breathing at 10 BPM. **d** Spontaneous breathing

Table 1 Error analysis for guided breathing tests. Absolute error is expressed in BPM, relative error reported in parenthesis

RR [BPM]	Nasal			Oral		
	6	8	10	6	8	10
Bias	0.1 (1.8%)	0.1 (1.5%)	0.2 (1.5%)	− 0.9 (− 27.4%)	− 1.9(− 39.4%)	− 2.0(− 34.8%)
Bias 95% CI	[0.06, 0.16]	[0.06, 0.18]	[0.11, 0.20]	[− 1.86, 0.06]	[− 3.11, − 0.75]	[− 3.50, − 0.49]
Precision	0.2 (3.4%)	0.3 (3.3%)	0.3 (2.8%)	2.3 (61.0%)	2.8 (60.2%)	3.6 (62.7%)
Accuracy	0.2 (3.8%)	0.3 (3.6%)	0.3 (3.2%)	2.5 (66.9%)	3.4 (72.0%)	4.1 (71.7%)

CI confidence interval

by the TRMS and by visual counting, is reported in Fig. 8a. The TRMS closely follows the reference values during the entire time frame of the spontaneous breathing experiment. To assess the agreement between the TRMS and the visual-count reference, a Bland-Altman plot for the representative subject is included in Fig. 8b, where the mean RR difference

is − 0.04 BPM, the standard deviation is 0.4 BPM, and the 95% confidence interval is [− 0.8, 0.7] BPM.

Bland-Altman analysis was also performed for the whole sample of volunteers (N = 20) under spontaneous breathing, whose results are included in Fig. 9. In this case, the mean and standard deviation of the RR difference
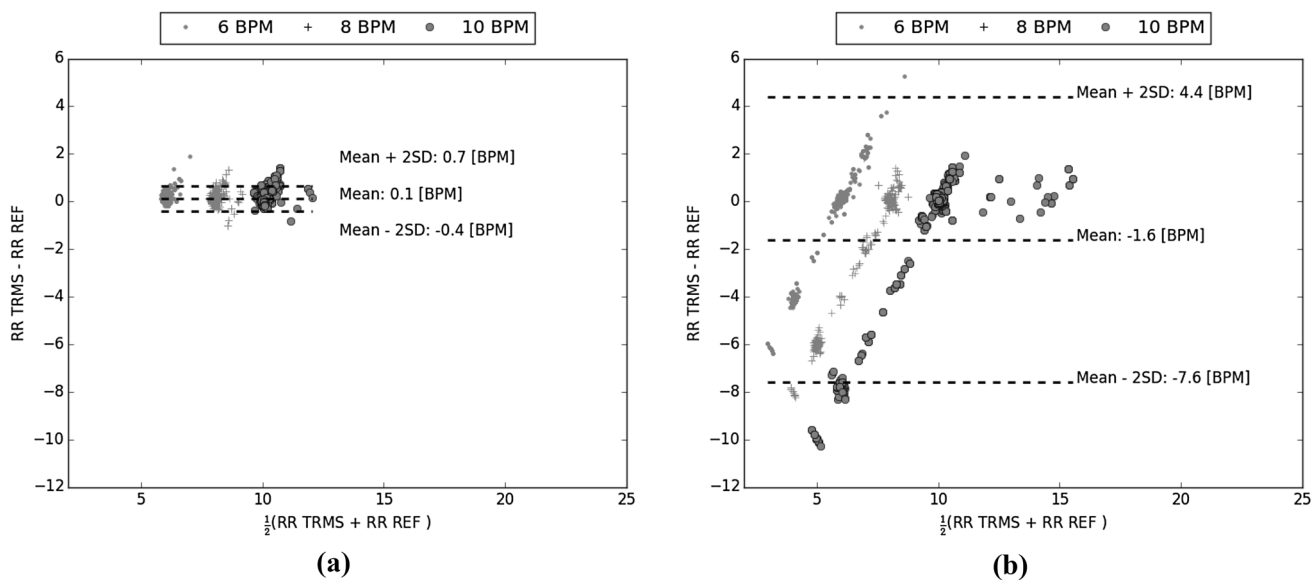
Fig. 7 Bland Altman plots for guided respiration tests. **a** Nasal breathing. **b** Oral breathing
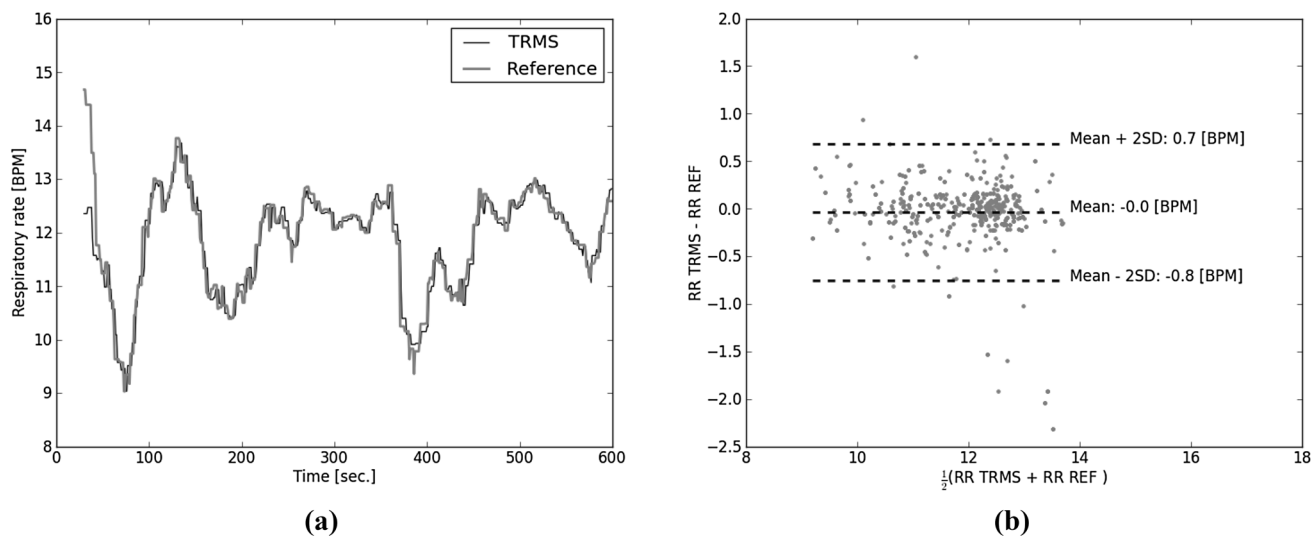

Fig. 8 Results for the spontaneous breathing test for a representative subject. **a** Respiratory rate evolution in time for the TRMS and the reference method (visual counting). **b** Bland-Altman plot for assessing the agreement of RR [BPM] measured by TRMS and the reference method

between the TRMS and the reference method for the group was 0.4 BPM and 0.45 BPM, respectively. The 95% confidence interval for the average RR difference was [− 0.5, 1.3] BPM.

The time evolution of the TRMS signal and RR, and the peripheral oxygen saturation (SpO2) measured by pulse oximetry in subject 7 for the erratic breathing test is reported in Fig. 10a. From the respiratory signal, a plateau is found in the time interval [60,90], which corresponds to a breath hold of roughly 30 s. During that time frame, the RR measured by the TRMS reached 5 BPM only 15 s after respiratory

flow was held, whereas the SpO2 was above 98% during the entire time frame analyzed.

During the spontaneous breathing study of subject 6, apnea events not directed by the examiner were captured both by the TRMS system and by visual counting when the patient fell asleep. The TRMS signal and RR, and the peripheral oxygen saturation (SpO2) measured by pulse oximetry for subject 6 are reported in Fig. 10b. Three apnea events were recognized from the respiratory signal, where plateaus are clearly identified. The RR measured by the TRMS fell down to 6 BPM during the three apnea events
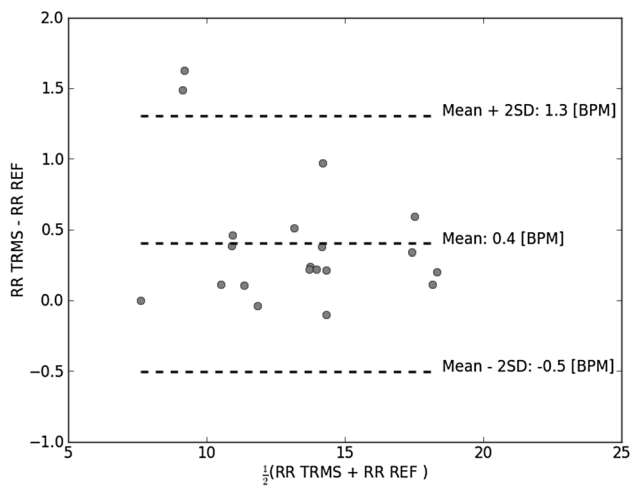
Fig. 9 Subject group Bland-Altman plot for assessing the agreement of RR [BPM] measured by the TRMS and the reference method

identified. The SpO2 was above 95% during the whole duration of the study, but some oscillations were observed, which seemed to be temporally correlated to the TMRS RR signal.

4 Discussion

In this work we have presented a novel temperature-based respiratory monitoring system. A novel concept in the TRMS is the thermal collector included in the respiratory sensor, made of a thermally-conductive material facing the respiratory gas entering and leaving the nose and mouth. From our study on the position sensitivity for nasal breathing, we

confirmed that the TRMS sensor provides a positive SNR for a larger region of placement than that delivered by standard thermistor, significantly outperforming standard thermistors when subject to misplacement. This enhanced performance of the TRMS is also reflected by accuracy values that were considerably smaller than those delivered by the thermistor system. These findings suggest that the TRMS can robustly measure nasal respiratory signal and RR more accurately than standard thermistors for a variety of positions, which highlights the robustness of the TRMS to accidental misplacement during installation.

Spontaneous-breathing tests showed that the TRMS provides an accurate estimate of the RR when compared to visual-based RR estimates. In the sample group, the mean RR difference obtained from the TRMS was 0.4 ± 0.45 BPM (equivalently, bias = 0.4 BPM, precision = 0.45 BPM, and accuracy = 0.36 BPM), which is comparable with studies using an electrical-impedance monitor on healthy subjects [19], a piezo-electric based monitor on PACU patients [13], and a photo-pletismography-based monitor on healthy subjects [1] reported in the literature, where the mean RR difference were 0.1 ± 0.17 BPM, 0.41 ± 1.79 BPM and 0.23 ± 1.14 BPM, respectively. While the mean RR difference obtained with the TRMS is at the upper end of these values, we note that the standard deviation is at the lower end, supporting the good precision in estimating RR provided by the TRMS. Further, we note that a small standard deviation directly impacts the 95% confidence interval for the mean RR difference, which in our case was $[-0.8, 0.7]$ BPM. The length of this confidence interval is significantly below 3 BPM, which has been used as a measure to classify RR estimates as
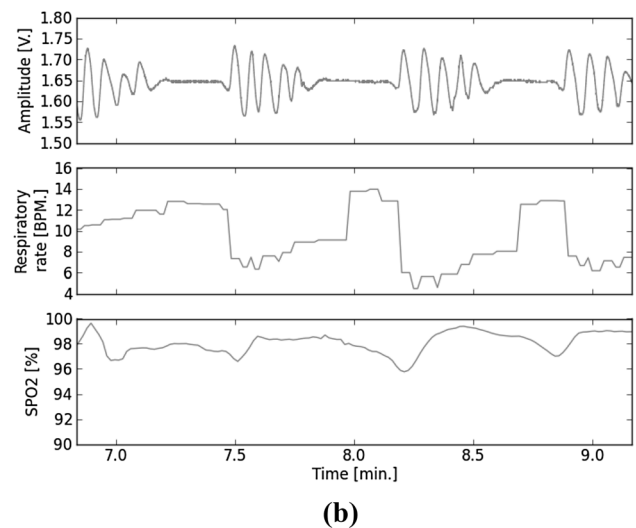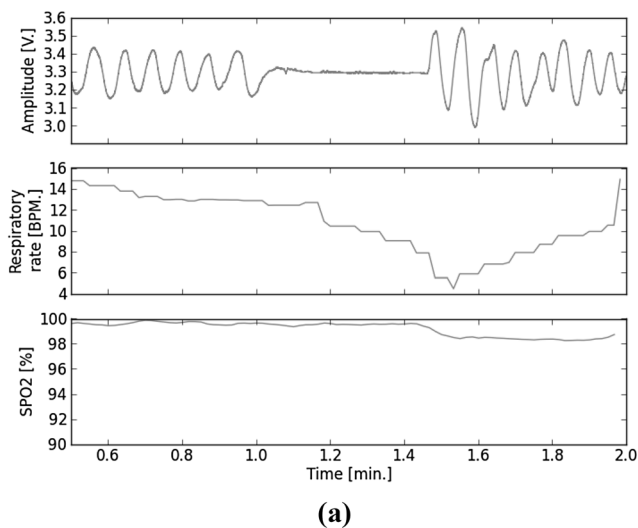

(a)

(b)

Fig. 10 Results for erratic breathing conditions. **a** Time evolution of TRMS signal amplitude, respiratory frequency and pulse-oximeter SpO2 for subject 7 under simulated apnea (controlled breath hold). **b**

Time evolution of TRMS signal amplitude, respiratory frequency and pulse-oximeter SpO2 for subject 6 during a spontaneous apnea event

clinically relevant [13]. RR estimates obtained by the TRMS in spontaneous breathing subjects are, in general, significantly more accurate than those based on visual imaging (bias = 4.72 BPM [18]), near infra-red imaging (accuracy = 1.12 BPM [14]), and infrared thermography (bias = 1.75 BPM [9]).

From the erratic breathing tests we conclude that the TRMS is capable of detecting when respiratory flow stops by using a threshold on the RR signal (RR < 6 BPM). Such approach was able to capture breath hold conditions in healthy subjects with a latency no larger than 20 s. In all subjects, SpO2 during such trained apnea events was very steady, and never reached saturation values below 95%. An interesting observation is the case of one patient who developed spontaneous apnea events while asleep. In that case, the TRMS was able to accurately detect such events, which suggest that the TRMS has a potential in alerting apnea events. Further studies that focus on sleep apnea and respiratory depression should be carried out to evaluate in depth this clinical application for the TRMS.

An important limitation of this study was the lower performance of the oral sensor in estimating RR, as evidenced by the controlled-breathing experiments where the maximum error bias was − 2.0 BPM, which is large when compared to the maximum bias of 0.2 BPM obtained for the nasal breathing case. Future developments of the TRMS should improve the temperature-based signal in order to decrease the measurement error. This finding notwithstanding, we note that the lower performance of the oral sensor does not adversely affect the TRMS estimate of the RR for spontaneous breathing, which can be nasal or oral. Future studies should also focus on validating the performance of the TRMS in patients in a clinical setting, such as the PACU, in order to confirm the applicability of our system to clinical respiratory monitoring purposes.

Compliance with ethical standards

Conflict of interest Authors declare no conflict of interest.

Ethical approval All procedures performed in studies involving human participants were in accordance with the ethical standards of the institutional ethics committee of the Pontificia Universidad Católica de Chile (Project ID 170523007, approved October 19th, 2017). All subjects provided written informed consent to participate.

References

1. Addison PS, Watson JN, Mestek ML, Mecca RS. Developing an algorithm for pulse oximetry derived respiratory rate (RRoxi): a healthy volunteer study. J Clin Monit Comput. 2012;26(1):45–51.
2. Addison PS, Watson JN, Mestek ML, Ochs JP, Uribe Alberto A, Bergese Sergio D. Pulse oximetry-derived respiratory rate in general care floor patients. J Clin Monit Comput. 2014;29(1):113–20.
3. Cavalcante AN, Martin YN, Sprung J, Imsirovic J, Weingarten TN. Low minute ventilation episodes during anesthesia recovery following intraperitoneal surgery as detected by a non-invasive respiratory volume monitor. J Clin Monit Comput. 2017;32(5):929–35.
4. Cretikos MA, Bellomo R, Hillman K, Chen J, Finfer Simon, Flabouris Arthas. Respiratory rate: the neglected vital sign. Med J Aust. 2008;188(11):657–9.
5. Dahan A, Aarts L, Smith TW. Incidence, reversal, and prevention of opioid-induced respiratory depression. Anesthesiology. 2010;112(1):226–38.
6. Folke M, Cernerud L, Ekström M, Hök B. Critical review of non-invasive respiratory monitoring in medical care. Med Biol Eng Comput. 2003;41(4):377–83.
7. Güder F, Ainla A, Redston J, Mosadegh B, Glavan Ana, Martin TJ, Whitesides George M. Paper-based electrical respiration sensor. Angewandte Chemie Int Ed. 2016;55(19):5727–32.
8. Guechi Y, Pichot A, Frasca D, Rayeh-Pelardy F, Lardeur Jean-Yves, Mimoz Olivier. Assessment of noninvasive acoustic respiration rate monitoring in patients admitted to an emergency department for drug or alcoholic poisoning. J Clin Monit Comput. 2015;29(6):721–6.
9. Hochhausen N, Barbosa Pereira C, Leonhardt S, Rossaint R, Czaplik Michael. Estimating respiratory rate in post-anesthesia care unit patients using infrared thermography: an observational study. Sensors. 2018;18(5):1618.
10. Hogan J. Why don't nurses monitor the respiratory rates of patients? Br J Nurs. 2006;15(9):489–92.
11. Knaus WA, Zimmerman JE, Wagner DP, Draper EA, Lawrence DE. APACHE-acute physiology and chronic health evaluation: a physiologically based classification system. Crit Care Med. 1981;9(8):591–7.
12. Lee LA, Caplan RA, Stephens LS, Posner KL, Terman Gregory W, Voepel-Lewis Terri, Domino Karen B. Postoperative opioid-induced respiratory depression. Anesthesiology. 2015;122:659–65.
13. Lee PJ. Clinical evaluation of a novel respiratory rate monitor. J Clin Monit Comput. 2016;30:175–83.
14. Li MH, Yadollahi A, Taati B. Noncontact vision-based cardiopulmonary monitoring in different sleeping positions. IEEE J Biomed Health Inform. 2017;21(5):1367–75.
15. Loughlin PC, Sebat F, Kellett JG. Respiratory rate: the forgotten vital sign - make it count!. Jt Comm J Qual Patient Saf. 2018;44(8):494–9.
16. Lu W, Nystrom MM, Parikh PJ, Fooshee DR, Hubenschmidt James P, Bradley Jeffrey D, Low Daniel A. A semi-automatic method for peak and valley detection in free-breathing respiratory waveforms. Med Phys. 2006;33(10):3634–6.
17. Mimoz O, Benard T, Gaucher A, Frasca D, Debaene B. Accuracy of respiratory rate monitoring using a non-invasive acoustic method after general anaesthesia. Br J Anaesth. 2012;108(5):872–5.
18. van Gastel M, Stuijk S, de Haan G. Robust respiration detection from remote photoplethysmography. Biomed Opt Express. 2016;7(12):4941–57.
19. Voscopoulos C, Brayanov J, Ladd D, Lalli M, Panasyuk Alexander, Freeman Jenny. Evaluation of a novel noninvasive respiration

monitor providing continuous measurement of minute ventilation in ambulatory subjects in a variety of clinical scenarios. Anesth Analg. 2013;117(1):91–100.

20. Wang S, Pohl A, Jaeschke T, Czaplik M, Köny M, Leonhardt S, Pohl N. A novel ultra-wideband 80 ghz fmcw radar system for contactless monitoring of vital signs. In: 2015 37th annual international conference of the IEEE engineering in medicine and biology society (EMBC). IEEE; 2015. pp. 4978–4981.

21. Zhang Xuezheng, Kassem Mahmoud Attia Mohamed, Zhou Ying, Shabsigh Muhammad, Wang Quanguang, Xuzhong Xu. A Brief Review of Non-invasive Monitoring of Respiratory Condition for Extubated Patients with or at Risk for Obstructive Sleep Apnea after Surgery. Frontiers in Medicine. 2017;4(March):1–6.